

Anisotropic polyurethane foam with Poisson's ratio greater than 1

Lee, T. and Lakes, R. S.,
"Anisotropic polyurethane foam with Poisson's ratio greater than 1",
Journal of Materials Science, 32, 2397-2401, (1997).

Abstract

Anisotropic polymer foams have been prepared, which exhibit a Poisson's ratio exceeding 1, and ratios of longitudinal to transverse stiffness exceeding 50. The foams are as much as 20 times stiffer in the longitudinal direction than the foams from which they were derived. The transformation process involved applying a uniaxial stress sufficient to produce 25% to 45% axial strain to open-cell polyurethane foam, heating above the softening point, followed by cooling under axial strain.

1. Introduction

A cellular material is one made up of an interconnected network of solid struts or plates which form edges and faces of cells. It may be viewed as a composite consisting of a solid phase and empty space or a fluid phase such as air. Cellular solids have served structural roles in nature as honeycombs, bone and coral skeletons, for millions of years. Man, on the other hand, has only recently begun to realize the potential of these materials and has made an attempt to utilize their structure-property relations in practical applications.

Cellular solids, including foams, are very efficient structures in terms of optimizing strength and stiffness with respect to weight. Foam materials have often been called "nature's equivalent of the I-beam" [1], and are commonly employed in cushioning, insulating, padding and packing et al. Encouraged by the engineering potential of cellular materials, one is motivated to understand the mechanical behavior of the cellular solid.

All commonly known cellular materials (naturally existing and man-made), have a convex cell shape and exhibit a positive Poisson's ratio which is defined as the negative of the lateral strain divided by the axial strain when a load is applied in an axial direction. Such materials undergo a lateral contraction in response to an axial stretch, and a lateral expansion when subjected to axial compression. Therefore, for all ordinary materials, Poisson's ratio has a positive value. For reference, typical Poisson's ratios for some common material are 0.5 for rubbers, 0.33 for aluminum, 0.27 for most steels, 0.1 to 0.4 for typical polymeric foams, and nearly zero for cork [2].

The theoretical allowable range of Poisson's ratio for isotropic materials in three dimensions is -1 to 0.5 as demonstrated by energy arguments [3]. An isotropic material with negative Poisson's ratio, however, was not believed to exist until recent work by Lakes [4]. The fabrication was achieved through a transformation of the cell structure from a convex polyhedral shape to a concave shape. These types of foam samples having a negative Poisson's ratio have been termed "re-entrant" due to their macrostructural appearance and behavior. Prior experiments in preparing and studying re-entrant polyurethane foam (Scott industrial foam) [4, 5, 6], silicone rubber foam [5] and metal foam [4, 5, 7] dealt with open-cell foam. Different techniques were used for each of these materials.

In this study, an open-cell polyurethane foam was strained in tension at elevated temperature, resulting in characteristic permanent transformations. Scott Industrial foam with a pore size 0.4 mm (65 pores per inch (ppi)) was used. This is similar, except for pore size, to the Scott foam (25 ppi) used in earlier studies of creation of negative Poisson's ratio foam [4, 5, 6]. This procedure resulted in completely different properties than those achieved in compressed

foams. Specifically, Poisson's ratios exceeding one were achieved. Moreover, substantial anisotropy in stiffness was generated.

2. Experimental procedure

2.1 Rationale

The Scott Industrial foam used in this study is a green polyurethane foam which has on average 65 pores per inch (ppi). From previous work, Scott foam of larger pore size [4] shows maximum re-entrant properties for final volumetric compression ratios of 3.3 to 3.7 [6]. Also, foam transformations at 170°C for 17 minutes gave rise to a minimum value of $\nu = -0.7$. These results, however, are based on a triaxial, mold compression procedure. In the present study, the Scott Industrial foam was placed under a uniaxial tension load and then, by heating and cooling, permanently deformed. Ultimately, it was desired to compare the mechanical properties (especially Poisson's ratio) of permanently stretched foam with triaxially compressed structures. In particular, it was anticipated that Poisson's ratio greater than 1/2 could be achieved.

2.2 Materials

The polyurethane foam [Scott Industrial foam, $\rho = 0.03 \text{ g/cm}^3$ (mass/volume), $\nu_s = 1.05 \sim 1.25 \text{ g/cm}^3$ for solid polyurethane [8], l (length of cell rib) = $0.4 \pm 0.03 \text{ mm}$] was obtained from Foamade Industries, Auburn Hills, MI, USA. The foam is reticulated with an open cell structure. The foam was provided in 2 meter lengths with a 5 cm \times 5 cm square cross-section. This material was then cut into lengths for specimens. There was some variation in the relative density in each bar, however, the variation was considered negligible. The specimens were made geometrically similar so that changes in strain rate with time would be similar for all samples.

2.3 Specimen preparation

The foam samples were cut into bars with dimensions of 5 cm \times 5 cm \times 30 cm. Holes were punched through two opposite sides of the foam, 5 cm from each end. Two 0.5" (12.7 mm) diameter bars were pushed through these holes and mounted to a constant-strain jig. Dimensional measurements for Poisson's ratio, ν , were taken for every 1 cm increment of axial displacement until the specimen failed. The oven was preheated to 30°C higher than the predetermined temperature (170°C) to compensate for a drop in temperature due to placement of the test jig. The samples were heated to a temperature in the range of 165°C \sim 175°C (via a mercury thermometer protruding from the oven top) for 17 minutes, as described in earlier studies of negative Poisson's ratio materials [4], [6]. The foam was then cooled to room temperature and the permanent strain was evaluated from dimensional measurements with a micrometer.

2.4 Scott foam test

Tensile tests were performed on the specimen with three settings of initial permanent strain: 0% (conventional or control), 25%, 35%, and 45%. Following procedures similar to those used in a prior study of conventional and re-entrant foam [6], the present foams were studied over a range of testing strains. For conventional Scott Industrial foam, Poisson's ratio increases rapidly under 25% \sim 45% tensile strain, with a maximum of $\nu = 0.55$ at $\epsilon = 45\%$. Any further increase in strain results in a gradual decrease in Poisson's ratio from its peak value. It was decided to produce permanent transformation strain from 25% \sim 45%, since this region in the nonlinear behavior of conventional foam [6] produces a rapid change in Poisson's ratio with increasing strain. Three experiments with each strain value of foam were performed, the summarized data are plotted in the Results and Discussion section.

Fiduciary marks were made for displacement evaluation using a fine, indelible marker near the center of each specimen; the marks were made sufficiently far from the ends that the strain field would be uniform by virtue of Saint Venant's principle. These gauge lines were drawn in the middle of one side of the specimen; 4 cm apart in the longitudinal direction and 2 cm apart in the

transverse direction. Another set of lines for use in measuring both longitudinal and transverse strains was drawn on an adjacent face of the sample. Incremental differences in the spacing of the gauge lines were measured to calculate longitudinal and transverse strains to infer Poisson's ratio of the foam.

The top of each marked line was used as a reference point for measurement to minimize error. Although the measurements were taken with special care, the results showed errors at small strains. This can be attributed in part to the limiting resolution of one's eye (0.1 mm) in comparison with the size of the open cell structure of the foam specimen and the size of the ink marks. The calculated Poisson's ratio values had higher error for lower strain due to uncertainty in measured displacement; these errors were plotted as error bars in Fig. 1.

Engineering stress-strain curves were plotted from the load-displacement data. These tests were performed with the use of several dead weights suspended from the end of the specimen. The weights were converted to metric (N) and original cross-sectional area (A_0) was calculated from the bar dimensions. The strains () in the direction of the applied load for each weight were plotted with stress ($P(N)/A_0$).

Both tensile and compression tests of all samples were performed to observe the mechanical behavior of the specimens. The modulus of elasticity of the material at small strains can be taken as the tangent modulus, E_t . In tensile tests, several data points were obtained for each sample's - curve. The tangent modulus, E_t , was taken between the origin and the first data point. The secant modulus, E_s , was found as the slope between the origin and the last data point. In compression tests, the final incremental load added to the column where buckling occurred was considered the critical buckling load. A 15-cm test section was cut from the middle of the sample, to avoid inhomogeneities caused by end effects. All of these columns were made geometrically similar, since the height of a column is inversely proportional to the square of the critical Euler buckling load.

In this study, the Young's modulus of each foam was already analyzed by virtue of its stress-strain curve. Also, the force causing catastrophic buckling to the column specimen was used to calculate the buckling strain in accordance with Hooke's law.

2.5 SEM evaluation of foams

The transformed and nontransformed Scott Industrial foams (polyurethane) were used in Scanning Electron Micrograph (SEM) evaluation ($\times 80$). The transformed foams used in this analysis were subjected to a uniaxial tension as a result of permanent tensile strains of 25%, 35%, and 45% respectively. These pictures show the types of cell microstructure present in these foams. A Hitachi "Nature" SEM (Model No. S-2460N at Central Electron Microscopy Research Facility) was used for the study. The term "Nature" refers to a variable pressure inside the specimen chamber. An accelerating voltage of 3 keV was used to take micrographs of the samples which were sputter-coated with Au-Pd.

3. Results and Discussion

The Poisson's ratio versus engineering strain for the control and permanently stretched foam samples (for both sides) with 25%, 35%, and 45% strains are plotted in Fig. 1. Both adjacent sides of samples (Side A, Side B) show agreement with data points from Poisson's ratio measurements within the error bars. Therefore only data points from side A measurements were plotted in Fig. 1 to reduce the complexity of the figure. The control specimens exhibit a Poisson's ratio near 0.3 for lesser tensile strain and exceeds, then approaches, a value of 0.5 in tension, at large strain. A Poisson's ratio of greater than 0.5 does not violate any physical laws, but illustrates a possible anisotropic behavior due to the large strains causing alignment of cell ribs. The permanently deformed foam samples indicate similar behaviors, in which the Poisson's ratios were near 1.1 initially for small tension strains, then approached 0.6 for large tension strains. A maximum of Poisson's ratio was found to be at a strain value around 0.04. After this maximum, the Poisson's ratio of permanently deformed foam samples tended to converge on a value range of

0.5 ~ 0.8. Both specimen types (control and deformed) show a converging Poisson's ratio for strains larger than 25%. Tension tests of deformed samples were limited to smaller strains, since the foam was observed to tear near the supports for strain levels in the gauge section beyond 0.3.

Calculations for error bars in Fig. 1 were based on (i) the uncertainty in evaluating the distance between two marks, and (ii) the uncertainty from the limiting resolution of one's eye (0.1 mm). Where no error bars are visible, the uncertainty is smaller than the resolution of the graphic data point. The error bars are larger at smaller strain values because the differences in ν between original and deformed samples are small.

The Poisson's ratio in the transverse (perpendicular to the load used to create permanent axial deformation) direction was found to be large at high tensile engineering strains. Large strains were needed in these tests since the transverse specimens were small, so that displacement for a given strain was smaller than in the case of the larger longitudinal specimens. Transverse plane Poisson's ratio values were measured to be approximately 1.5 at $\epsilon = 0.5$, in contrast to the Poisson's ratio of the control material: 0.5. The Poisson's ratio of the control material in the transverse plane was identical to the Poisson's ratio in longitudinal tests, confirming the isotropy of the unprocessed foam.

As for compression, the buckling strains exhibit decreasing values with increasing permanent strains. This behavior also can be explained by the reduction of resilience in samples processed at higher permanent strains. Actually it is simple. With processing, the stiffness increases due to cell rib alignment, but the collapse strength, governed by rib buckling, does not change much; consequently the strain associated with material buckling decreases with processing permanent strain.

Buckling in compression limited the measurements in compression since a measuring measurement of strain, needed to infer modulus and Poisson's ratio, can only be made under conditions of uniform strain in the gauge section. The buckling was an internal buckling (Fig. 2) rather than Euler column buckling. Buckling was observed even in very short specimens.

Band instability due to microbuckling has been seen previously in the plateau region of conventional foams [9]. Although those bands were of low contrast, presently observed specimen buckling is more macroscopic and more easily observable.

Engineering stress-strain curves for both longitudinal and transverse directions were evaluated from tensile tests of original and permanently stretched Scott Industrial foam samples. Resulting stress-strain curves for the axial (strained-tensional) direction are plotted in Fig. 3. Specimens with higher degrees of permanent strain, exhibited a higher stiffness and a lower strain value at failure. This phenomenon may be due to the fact that the highly stretched foam was already near the limitation of maximum strain for the foam material.

From the experimental stress-strain curve, the Young's modulus, E , was calculated via two graphical methods. The tangent modulus, E_t , is considered the slope of the line from the origin to the first data point. The secant modulus, E_s , was found as the slope of a line between the origin and a data point. For this comparison, the last data point in the series was used. These moduli are plotted in Fig. 4 versus permanent strain values. The longitudinal tangent modulus increased rapidly with the larger permanent strain values. These results, as inferred from the previous graph, show that the foam becomes stiffer in the axial (strained-tensional) direction by increasing the permanent strain value.

Fig. 5 shows the engineering stress-strain curves for tests measuring transverse sections of control and permanently stretched foams. As opposed to Fig. 3, stretched specimens with higher permanent strains show larger strain values at a given stress level. The transformed foam is anisotropic: it is much stiffer in the longitudinal direction than it is in the transverse direction.

Both secant and tangent moduli for the transverse direction were calculated from the data in the previous graph and displayed in Fig. 6. For a small strain range, data acquisition for tangent modulus was difficult due to a decrease of relative resolution. This problem was solved by using a "polynomial" function for curve fitting in the graphing software. Each stress-strain curve was considered as a quadratic function $\sigma = E_t \epsilon + A \epsilon^2$ and the value E_t from the curve-fit was used as

tangent modulus. Both mechanical moduli rapidly reduce with higher values of permanent strain in the foams. The transformed foam is considerably more compliant for tension in transverse directions than for the longitudinal direction (the direction of the permanent stretch).

Fig. 7 shows the micrograph of a control foam sample. The cells in this foam are rather round and symmetrical. It can be observed that cell ribs have a triangular cross-section. In comparison to the cellular structure in the control foam, the cells of the transformed foam are elongated and appear more irregular as shown in Fig. 8. In permanently stretched foam, cell ribs tend to align in one direction. Cell structures show sharp elliptical pores compared with the original foam. This type of combined deformation provides a reason for the small strain range observed in highly transformed specimens. Thus the SEM pictures confirm previous observations of mechanical anisotropy.

Foams which were transformed by permanent uniaxial stretching exhibited increased axial stiffness (by as much as a factor of 20), larger Poisson's ratio in excess of 1, and orientation of the microstructure. Poisson's ratios exceeding 1/2 are permissible in anisotropic materials. Indeed, hexagonal honeycombs can exhibit Poisson's ratio of 1, and if they have oriented hexagonal cells, greater than 1, in certain directions [2].

Materials with $> \frac{1}{2}$ in both transverse directions have been termed "stretch densifying" in the terminology of Baughman [10], who found certain (anisotropic) crystals to exhibit such a property. The present foams exhibit a controllable stretch-densifying property, achieved by processing. The present anisotropic foams are in contrast to the re-entrant foams developed by one of the authors [4]; these foams were produced by triaxial permanent compression, and they exhibited reduced Young's modulus, negative Poisson's ratio, and a micro-buckling of the microstructure due to the processing.

4. Conclusions

1. The Poisson's ratio of samples with 25%, 35%, and 45% permanent uniaxial strains was about 1.1 at small tensile strain. These foams exhibited maximum values of Poisson's ratio around 1.5 at a strain of 0.04. At higher strain, the Poisson's ratio of both transformed and control foams tended to converge on a value range of 0.5 ~ 0.8.
2. Compression experiments at small loads disclosed an internal banding form of buckling in permanently stretched foams.
3. The transformed foam becomes stiffer in the axial (strained-tensional) direction, by a factor of up to 20.
4. The values of secant and tangent modulus in the transverse direction of permanently stretched foams decrease with increasing permanent strain values. The transformed foam is considerably more compliant in tension, in transverse directions, than for longitudinal directions (the direction of the permanent stretch).
5. SEM pictures of permanently stretched polyurethane shows elongated and irregular cell structure than control foams. This deformation characteristic accounts for the anisotropy observed in highly transformed specimens.

Acknowledgements

Support of this research by the Boeing ACTAS program is gratefully acknowledged.

References

1. M. F. Ashby, The Mechanical properties of cellular solids, Metallurgical Transactions A, Vol. 14A, pp. 1755-1769, 1983
2. L. J. Gibson, M. F. Ashby, Cellular solids, Pergamon Press, Oxford, 1988
3. Y. C. Fung, Foundation of Solid Mechanics, Prentice-Hall, Englewood Cliffs, NJ, 1968
4. R. S. Lakes, Foam structures with a negative Poisson's ratio, Science, Vol. 235, pp. 1038-1040, 1987

5. E. A. Friis, R. S. Lakes, J. B. Park, Negative Poisson's ratio polymeric and metallic foams, *J. Mat. Sci.*, Vol. 23, pp. 4406-4414, 1988
6. J. B. Choi, R. S. Lakes, Non-linear properties of polymer cellular materials with a negative Poisson's ratio, *J. Mat. Sci.*, Vol. 27, pp. 4678-4684, 1992
7. J. B. Choi, R. S. Lakes, Non-linear properties of metallic cellular materials with a negative Poisson's ratio, *J. Mat. Sci.*, Vol. 27, pp. 5375-5381, 1992
8. *Modern Plastics Encyclopedia*, Vol. 51, No. 10A, 1974-1975
9. R. Lakes, P. Rosakis, A. Ruina, Microbuckling instability in elastomeric cellular solids, *J. Mat. Sci.*, Vol. 28, pp. 4667-4672, 1993
10. R. H. Baughman, D. S. Galvao, Crystalline networks with unusual predicted mechanical and thermal properties, *Nature*, Vol. 365, pp. 735-737, 1993

Figures

Figure 1 Poisson's ratio versus engineering strain for original and permanently stretched Scott Industrial foam samples; solid diamond represents internal buckling strain; Poisson's ratio not measured. Circles, squares, diamonds and triangles represent control, permanent strain values of 25%, 35%, and 45%, respectively.

Figure 2 Demonstration of the buckling in the permanently stretched Scott foam under compression

Figure 3 Engineering stress versus strain curve for original and permanently stretched Scott foam samples in longitudinal direction. Circles, squares, diamonds and triangles represent control, permanent strain values of 25%, 35%, and 45%, respectively.

Figure 4 Longitudinal Young's modulus versus permanent strain for original and permanently stretched Scott foam samples. Circles and squares represent secant and tangent modulus, respectively.

Figure 5 Engineering stress versus strain curve for original and permanently stretched Scott foam samples in transverse direction. Circles, squares, diamonds and triangles represent control, permanent strain values of 25%, 35%, and 45%, respectively.

Figure 6 Transverse Young's modulus versus permanent strain for original and permanently stretched Scott foam samples. Circles and squares represent secant and tangent modulus, respectively.

Figure 7 Scanning electron micrograph of conventional Scott Industrial foam. Magnification $\times 80$, accelerating voltage 3 keV.

Figure 8 Scanning electron micrograph of 45% permanently stretched Scott Industrial foam. Magnification $\times 80$, accelerating voltage 3 keV.

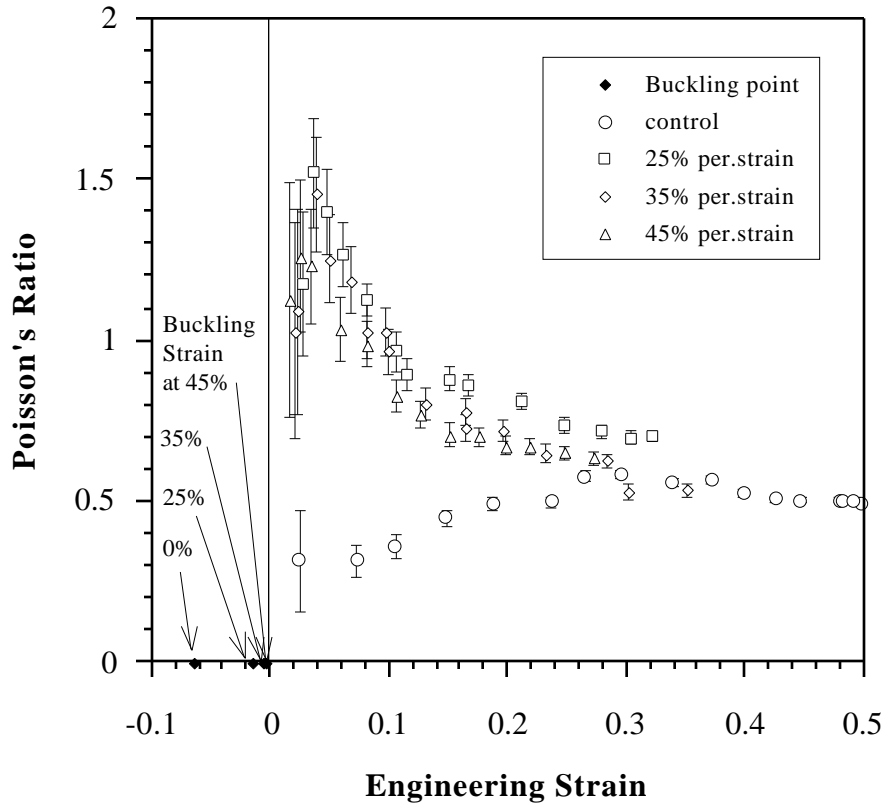


Figure 1 Poisson's ratio versus engineering strain for original and permanently stretched Scott Industrial foam samples; solid diamond represents internal buckling strain; Poisson's ratio not measured. Circles, squares, diamonds and triangles represent control, permanent strain values of 25%, 35%, and 45%, respectively.

Figure 2 Demonstration of the buckling in the permanently stretched Scott foam under compression

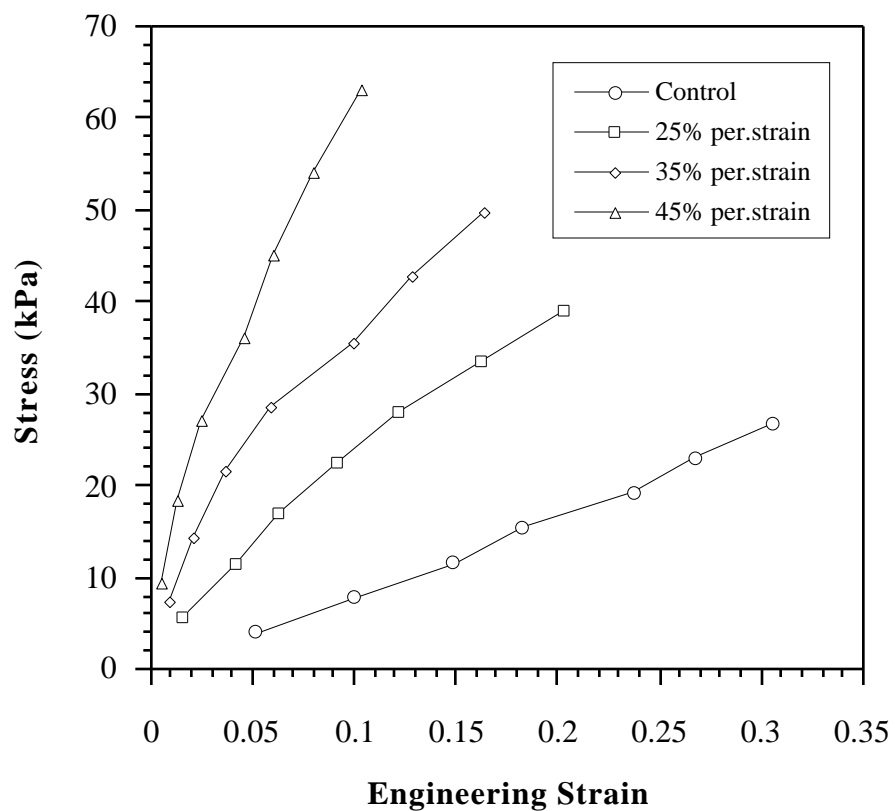


Figure 3 Engineering stress versus strain curve for original (control: zero permanent strain) and permanently stretched Scott foam samples in longitudinal direction. Circles, squares, diamonds and triangles represent control, permanent strain values of 25%, 35%, and 45%, respectively.

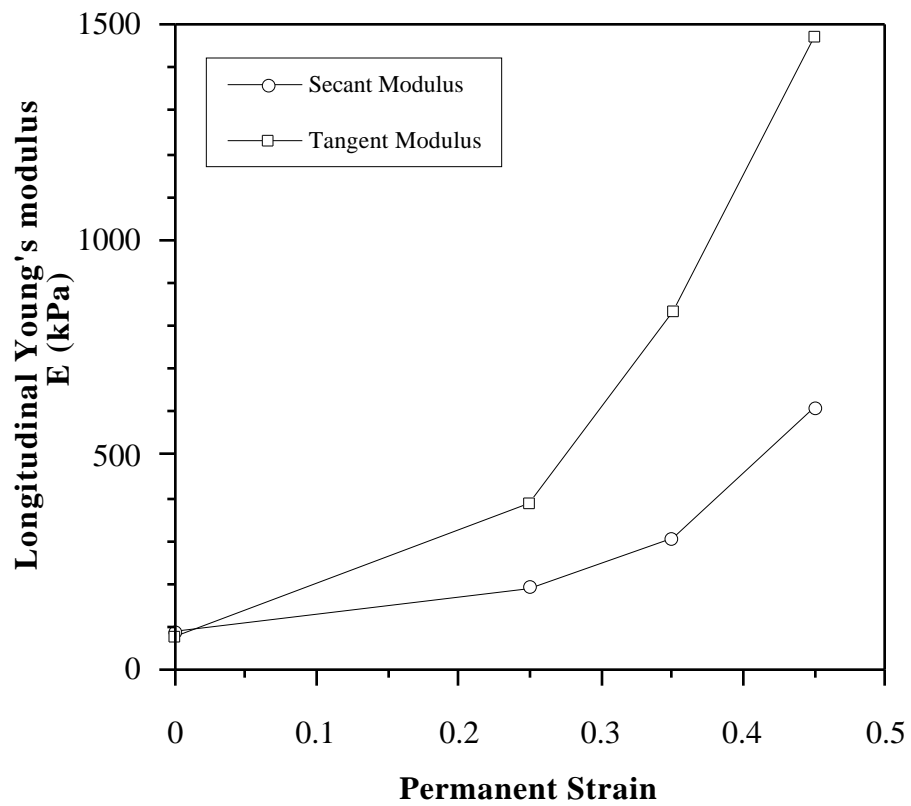


Figure 4 Longitudinal Young's modulus versus permanent strain for original (control: zero permanent strain) and permanently stretched Scott foam samples. Circles and squares represent secant and tangent modulus, respectively.

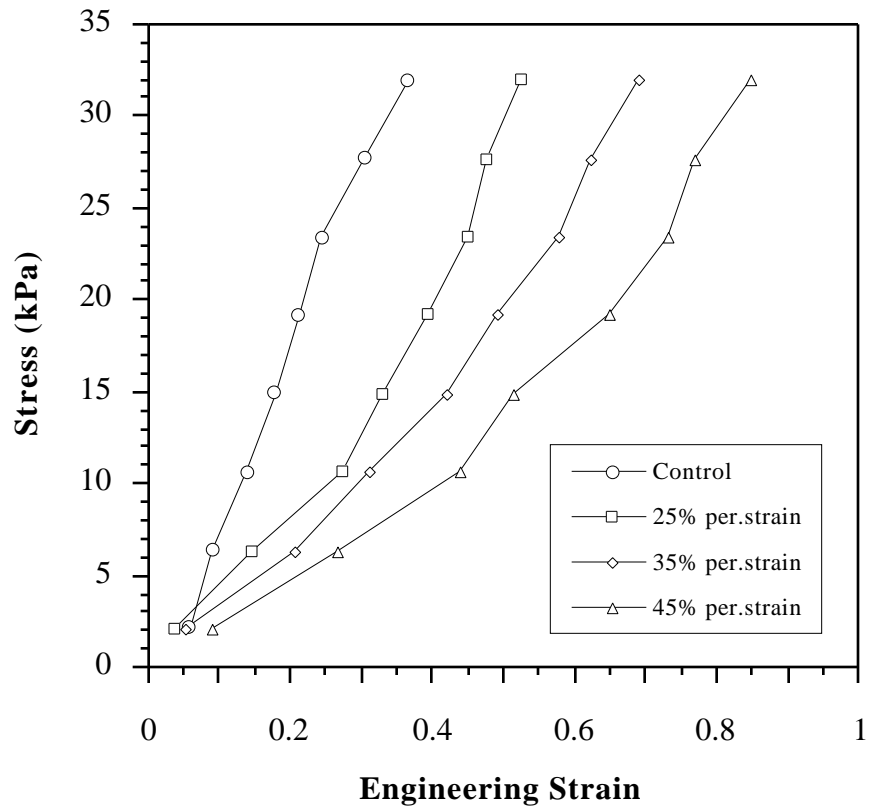


Figure 5 Engineering stress versus strain curve for original (control: zero permanent strain) and permanently stretched Scott foam samples in transverse direction. Circles, squares, diamonds and triangles represent control, permanent strain values of 25%, 35%, and 45%, respectively.

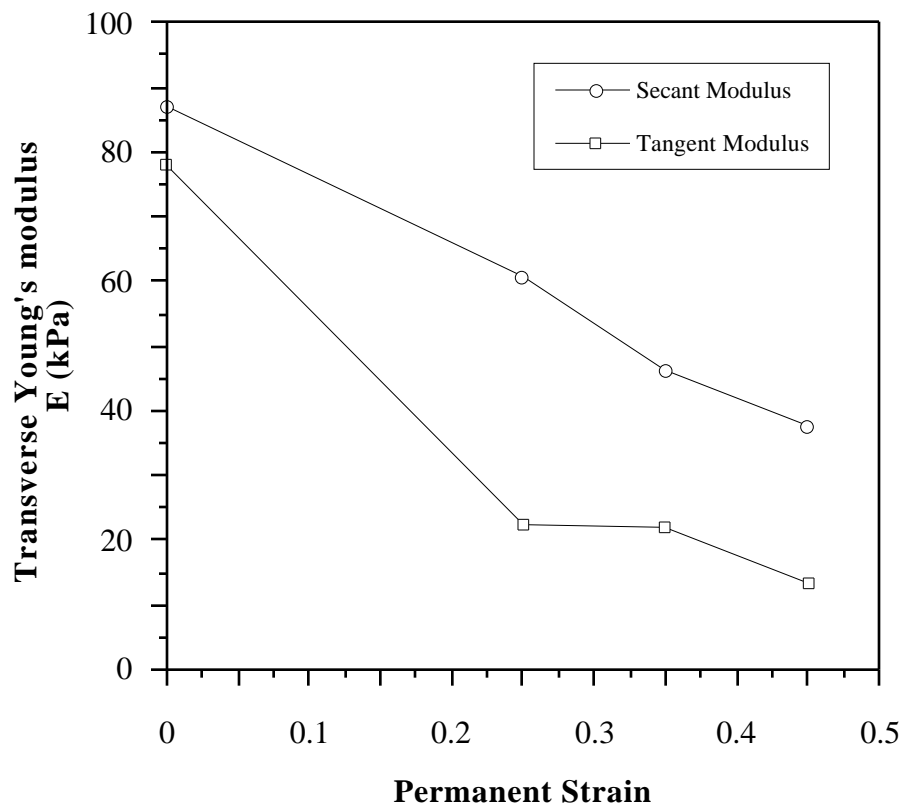


Figure 6 Transverse Young's modulus versus permanent strain for original (control: zero permanent strain) and permanently stretched Scott foam samples. Circles and squares represent secant and tangent modulus, respectively.

Figure 7 Scanning electron micrograph of conventional Scott Industrial foam. Magnification $\times 80$, accelerating voltage 3 keV.

Figure 8 Scanning electron micrograph of 45% permanently stretched Scott Industrial foam. Magnification $\times 80$, accelerating voltage 3 keV.